Nanobodies that block gating of the P2X7 ion channel ameliorate inflammation

Welbeck Danquah, Catherine Meyer-Schwesinger, Björn Rissiek, Carolina Pinto, Arnau Serracant-Prat, Miriam Amadi, Domenica Iacenda, Jan-Hendrik Knop, Anna Hammel, Philine Bergmann, et al.

DRUG DEVELOPMENT

Nanobodies that block gating of the P2X7 ion channel ameliorate inflammation

Welbeck Danquah,[1]*† Catherine Meyer-Schwesinger,[2]* Björn Rissiek,[1,3]* Carolina Pinto,[1] Arnau Serracant-Prat,[1] Miriam Amadi,[1] Domenica Iacenda,[1,3] Jan-Hendrik Knop,[1,2] Anna Hammel,[1,2] Philine Bergmann,[1,4] Nicole Schwarz,[1] Joana Assunção,[5]‡ Wendy Rotthier,[5] Friedrich Haag,[1] Eva Tolosa,[1] Peter Bannas,[1,6] Eric Boué-Grabot,[4] Tim Magnus,[3] Toon Laeremans,[5]§ Catelijne Stortelers,[5] Friedrich Koch-Nolte[1]||

Ion channels are desirable therapeutic targets, yet ion channel–directed drugs with high selectivity and few side effects are still needed. Unlike small-molecule inhibitors, antibodies are highly selective for target antigens but mostly fail to antagonize ion channel functions. Nanobodies—small, single-domain antibody fragments—may overcome these problems. P2X7 is a ligand-gated ion channel that, upon sensing adenosine 5′-triphosphate released by damaged cells, initiates a proinflammatory signaling cascade, including release of cytokines, such as interleukin-1β (IL-1β). To further explore its function, we generated and characterized nanobodies against mouse P2X7 that effectively blocked (13A7) or potentiated (14D5) gating of the channel. Systemic injection of nanobody 13A7 in mice blocked P2X7 on T cells and macrophages in vivo and ameliorated experimental glomerulonephritis and allergic contact dermatitis. We also generated nanobody Dano1, which specifically inhibited human P2X7. In endotoxin-treated human blood, Dano1 was 1000 times more potent in preventing IL-1β release than small-molecule P2X7 antagonists currently in clinical development. Our results show that nanobody technology can generate potent, specific therapeutics against ion channels, confirm P2X7 as a therapeutic target for inflammatory disorders, and characterize a potent new drug candidate that targets P2X7.

INTRODUCTION

Genetic and pharmacological studies in humans have implicated the adenosine 5′-triphosphate (ATP)–gated P2X7 ion channel as a therapeutic target in several inflammatory diseases, including glomerulonephritis, multiple sclerosis, and chronic pain (*1*–*4*). Consistently, studies with P2X7-deficient mice have also corroborated a key role of P2X7 in experimentally induced inflammatory diseases (*5*–*8*). P2X7 is prominently expressed by monocytes and T cells and responds to ATP released from damaged cells as a danger signal during inflammation (*9*, *10*). ATP-induced gating of P2X7 permits influx of calcium (Ca^{2+}) and sodium (Na^{+}) ions and efflux of potassium ions (K^{+}). P2X7 is a key player in the processing and release of the proinflammatory cytokine interleukin-1β (IL-1β) by lipopolysaccharide (LPS)–primed macrophages and is involved in the ectodomain shedding of membrane proteins and the externalization of phosphatidylserine by T cells (*9*, *11*, *12*).

Selective small-molecule inhibitors of P2X7 have been developed for the treatment of inflammatory diseases by Pfizer (CE-224,535), AstraZeneca (AZ-10606120 and AZD9056), and other pharmaceutical companies (*13*–*16*). Many of these P2X7 antagonists have shown promising results in preclinical trials of glomerulonephritis, multiple sclerosis, inflammatory pain, rheumatoid arthritis, and mood disorders (*13*–*18*). However, the two compounds tested in phase 2 clinical trials for rheumatoid arthritis, AZD9056 and CE-224,535, did not show any benefit beyond that of methotrexate (NCT00520572 and NCT00628095) (*19*, *20*). Additional trials with AZD9056 for osteoarthritis, chronic obstructive pulmonary disease, and Crohn's disease showed a benefit only in Crohn's disease (Eudra-CT2005-002319-26) (*21*). These studies illustrate the limitations of small-molecule P2X7 inhibitors, including a small therapeutic window, short in vivo half-life, side effects on other members of the P2X family, and conversion into ineffective and potentially toxic metabolites. Thus, an unmet medical need for potent, less toxic P2X7 antagonists remains (*15*, *18*).

Because of their exquisite specificity, low toxicity, and simple pharmacodynamics, antibodies are emerging as a potent class of therapeutics in autoimmunity, cancer, and infection. They are large, tetrameric proteins of ~150 kDa that do not pass the renal filtration barrier and therefore exhibit a much longer half-life (>10 days) than small-molecule drugs. Current anti-inflammatory antibodies are directed against cytokines, cytokine receptors, and cell-cell interaction molecules. Although ion channels are potential therapeutic targets on immune cells for inflammatory diseases, they have remained underexplored as targets of antibody therapeutics (*22*). Although conventional antibodies can diminish ion channel function by inducing endocytosis, they rarely directly interfere with ion channel function (*22*). Because of a unique propensity to bind functional crevices on proteins (*23*), nanobodies may fulfill the need for highly specific therapeutics toward ion channels (*24*, *25*).

Nanobodies are therapeutic proteins based on the smallest antigen-binding domains of naturally occurring heavy chain–only antibodies from camelids. These single-domain antibodies are $^{1}/_{10}$ the size of conventional antibodies and exhibit many advantages over conventional antibodies (*26*, *27*). With a long flexible CDR3 loop, nanobodies can bind conformational epitopes that are inaccessible to conventional

[1]Institute of Immunology, University Medical Center Hamburg-Eppendorf, Martinistraße 52, D-20246 Hamburg, Germany. [2]Department of Nephrology, University Medical Center Hamburg-Eppendorf, Martinistraße 52, D-20246 Hamburg, Germany. [3]Department of Neurology, University Medical Center Hamburg-Eppendorf, Martinistraße 52, D-20246 Hamburg, Germany. [4]Université de Bordeaux, Institut des Maladies Neurodégénératives, CNRS UMR 5293, Bordeaux 33076, France. [5]Ablynx NV, Technologiepark 21, B-9052 Zwijnaarde, Belgium. [6]Department of Radiology, University Medical Center Hamburg-Eppendorf, Martinistraße 52, D-20246 Hamburg, Germany.
*These authors contributed equally to this work.
†Present address: Evotec AG, Essener Bogen 7, 22419 Hamburg, Germany.
‡Present address: FairJourney Biologics, Rua do Campo Alegre 1021, 4169-007 Porto, Portugal.
§Present address: Confo Therapeutics, Pleinlaan 2, 1050 Brussels, Belgium.
||Corresponding author. Email: nolte@uke.de

antibodies, such as the cryptic active site of an enzyme (*24*, *25*). Moreover, the single-domain format of nanobodies facilitates the construction of multispecific and multivalent biologics by genetically linking nanobodies in a linear fashion (*25*, *27*). In vivo, monomeric nanobodies penetrate tissues better and more rapidly than conventional antibodies but are swiftly eliminated by renal filtration. The in vivo half-life of mono- or multivalent nanobodies can be tuned, for instance by genetic fusion to an albumin-specific nanobody (*28*). Similarly, genetic fusion with targeting moieties of Fc domains can endow nanobodies with additional effector functions, from translocation across the blood-brain barrier to cytotoxicity (*25*, *29*).

We hypothesized that nanobodies could be tailored to modulate P2X7 function on macrophages and T cells in vivo and thereby provide therapeutic benefit in inflammatory diseases. We set out to generate highly specific P2X7 nanobodies (both antagonists and potentiators of P2X7 function) and test their efficancy in models of inflamation.

RESULTS

Immunization of llamas with P2X7 in native conformation yields potent functional nanobodies

To present the P2X7 ion channel in its native conformation to cells of the llama immune system, we applied two immunization strategies: human embryonic kidney (HEK) cells stably expressing P2X7 for one group of llamas (mouse P2X7) and intradermal complementary DNA (cDNA) immunizations with a gene gun followed by a boost with P2X7-transfected HEK cells for a second group of llamas (mouse P2X7 and human P2X7) (Fig. 1A). Both groups showed P2X7-specific antibody responses (Fig. 1B). To select nanobodies that recognize native mouse P2X7, we cloned nanobody-phage display libraries from the immunized animals and panned these libraries on P2X7-expressing cells. Sequence analyses of selected target-binding clones revealed enrichment of 18 nanobody families (table S1).

To evaluate the capacity of nanobodies to modulate the function of P2X7, we used nucleotide-induced ectodomain shedding of CD62L by Yac-1 mouse lymphoma cells as a convenient readout (fig. S1). Nanobodies from six distinct families either blocked or enhanced both ATP-mediated and nicotinamide adenine dinucleotide (NAD^+)–mediated activation of P2X7. The most potent blocker, nanobody 13A7 [median inhibitory concentration (IC_{50}), 12 nM], and the most potent enhancer, nanobody 14D5 [median effective concentration (EC_{50}), 6 nM], were selected for further analyses. Flow cytometric analyses with transfected HEK cells verified specific binding of these nanobodies to mouse P2X7 but not to human P2X7, mouse P2X1, or mouse P2X4 (Fig. 1C).

Dimerization enhances the potency of P2X7-modulating nanobodies

The single-domain format of nanobodies facilitates their assembly into dimers and multimers. Because P2X7 is a homotrimeric ion channel, we reasoned that dimerization of nanobodies would improve binding affinity and enhance functional potencies. Thus, we generated dimeric molecules of nanobodies 13A7 and 14D5 by genetically fusing two single domains via a flexible peptide linker (Fig. 2, A and B). To provide half-life extension (HLE) for in vivo applications, we genetically fused homodimers of 13A7 and 14D5 to the albumin-binding nanobody Alb8, which causes the fused product to adopt the serum half-life of albumin in the respective host species (*28*). We also reconstituted a bivalent heavy chain antibody format by genetically fusing

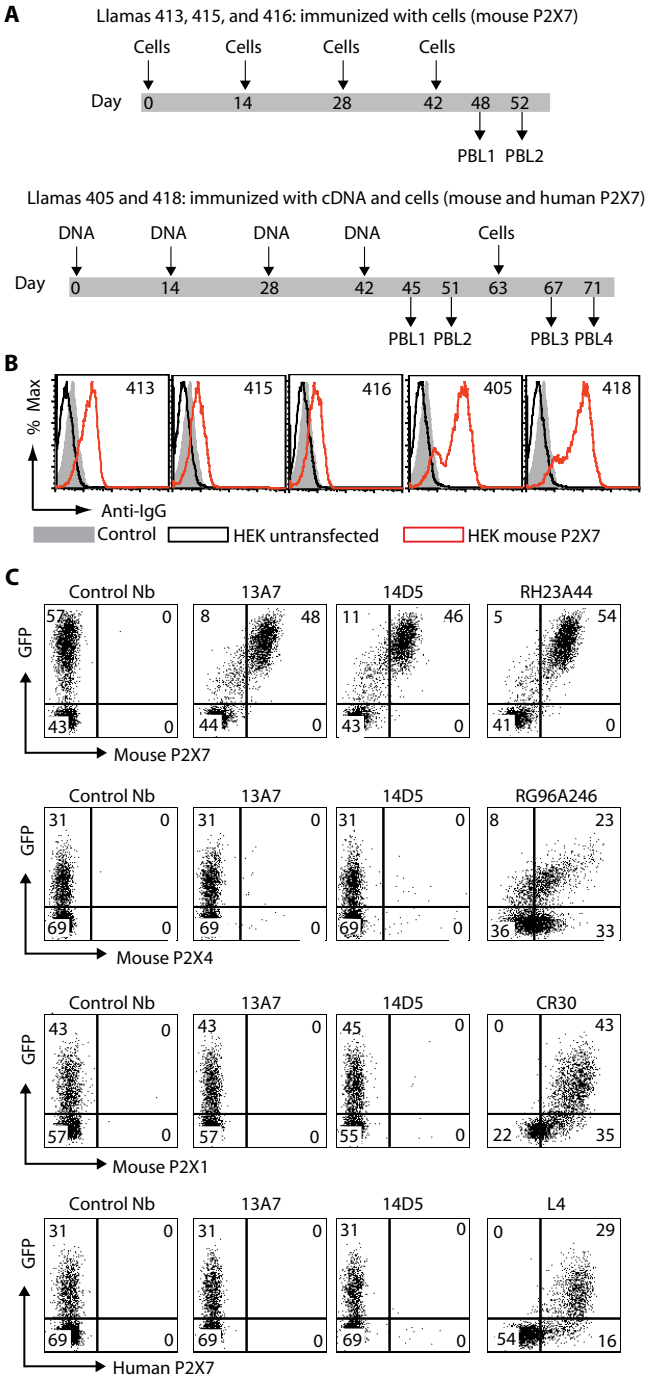

Fig. 1. Selection of P2X7-specific nanobodies from immunized llamas. (**A**) Llamas 413, 415, and 416 were immunized with P2X7-transfected HEK cells. Llamas 405 and 418 were immunized with a P2X7 cDNA expression vector and were boosted once with P2X7-transfected HEK cells. The VHH repertoire was cloned from peripheral blood lymphocytes (PBLs) prepared 3 to 10 days after the fourth and fifth boosts. (**B**) Flow cytometric analyses of the reactivity of llama immune sera obtained after the last boost with untransfected and with mouse P2X7–transfected HEK cells. IgG, immunoglobulin G. (**C**) Flow cytometric analyses of the reactivity of Nb-Fc fusion proteins with HEK cells co-transfected with green fluorescent protein (GFP) and mouse P2X7, mouse P2X4, mouse P2X1, or human P2X7. Control staining was performed with the indicated conventional antibodies directed against mouse P2X1 (CR30), mouse P2X4 (RG96A246), mouse P2X7 (RH23A44), or human P2X7 (L4). Data are representative of two (B) or three (C) independent experiments.

the nanobodies to the hinge and Fc domains of mouse IgG2c. Comparative dose-response analyses of monomeric 13A7 and 14D5 and their dimeric counterparts revealed 7- to 50-fold increases in P2X7-blocking and P2X7-enhancing potencies, respectively (Fig. 2, C and D). The three different versions of bivalent nanobodies—nanobody-dimers, HLE-dimers, and Fc fusions (Nb-Fc)—showed similar potencies. The 13A7 Nb-Fc format, a reconstituted heavy chain antibody, was more than 100 times more potent than four previously described P2X7-specific monoclonal antibodies (*30*–*32*) in blocking ATP-induced shedding of CD62L by mouse T cells (Fig. 2E).

Bivalent nanobodies modulate ATP-induced ion channel function in P2X7-expressing cells

Binding of extracellular ATP gates the P2X7 ion channel, resulting in a sustained influx of Ca^{2+} and Na^+ and an efflux of K^+. To measure the effect of P2X7-blocking (13A7) and P2X7-potentiating (14D5) nanobodies on ATP-induced P2X7 currents, we performed two-electrode voltage-clamp recordings on mouse P2X7–expressing *Xenopus* oocytes (Fig. 3A). Oocytes responded to the application of ATP with the characteristic slow and sustained currents in the presence of control Nb-Fc fusion proteins. In the presence of 13A7-Fc, ATP application induced little, if any, detectable currents. In contrast, in the presence of 14D5-Fc, ATP-evoked currents displayed faster activation and higher current amplitudes.

In P2X7-transfected HEK293 cells, nanobody 13A7-dimer effectively blocked ATP-induced Ca^{2+} influx, whereas 14D5-dimer potentiated ATP-induced Ca^{2+} influx in these cells and sustained Ca^{2+} influx even in response to low, subthreshold concentrations of ATP (Fig. 3B). When added to cells already showing sustained ATP-induced Ca^{2+} influx, 13A7-dimer reversed Fluo-4 (Ca^{2+} indicator) signals, whereas 14D5-dimer further potentiated these signals (Fig. 3C). Nanobody titration analyses revealed a dose-dependent blockade of P2X7, with similar subnanomolar IC_{50}/EC_{50} values for blockade/potentiation of both ATP-induced Ca^{2+} influx (Fig. 3D) and ATP-induced shedding of CD62L (Fig. 2D), confirming that nanobodies block different downstream effects of P2X7.

Monovalent and bivalent nanobodies 13A7 and 14D5 also effectively blocked or potentiated ATP-induced pore formation (fig. S2A). The effects of monovalent nanobodies 13A7 and 14D5 were readily reversed when cells were washed, whereas bivalent nanobodies showed continued functional effects even after washing, consistent with a slower rate of dissociation of bivalent nanobodies (fig. S2A). Further pharmacological characterization showed that the small-molecule P2X7 antagonist A438079 and nanobody 13A7 both blocked the potentiating effect of nanobody 14D5 on ATP-induced Ca^{2+} influx (fig. S2B). Moreover, nanobodies 13A7 and 14D5 also respectively blocked and potentiated gating of P2X7 by BzATP [2′(3′)-*O*-(4-benzoylbenzoyl)ATP], a P2X7-specific agonist (fig. S2C), underscoring their specificity toward P2X7.

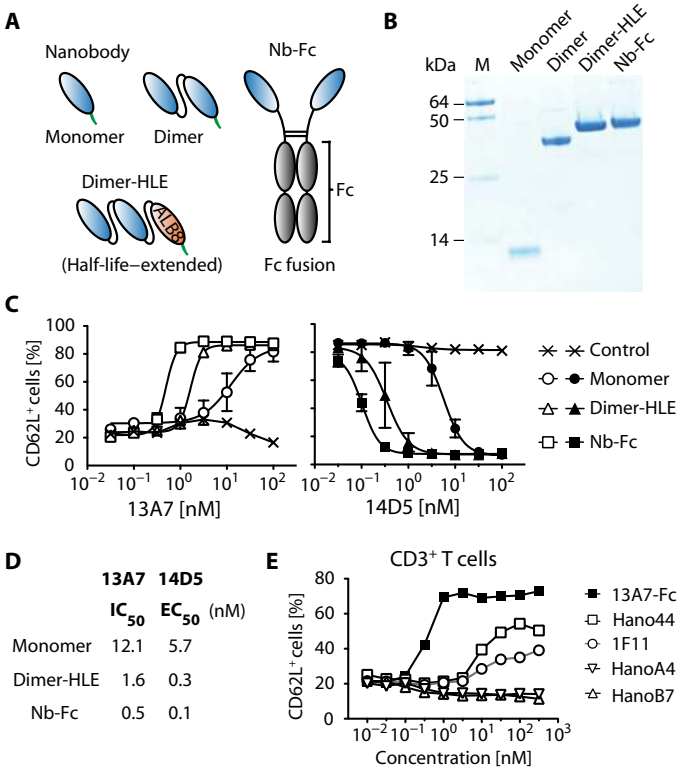

Fig. 2. Bivalent nanobodies exhibit higher potencies than monovalent nanobodies and conventional monoclonal antibodies. (**A**) Schematic diagram of monovalent and reformatted bivalent Nanobodies. Blue, anti-P2X7 nanobodies; orange, antialbumin nanobody Alb8; green, C-terminal *c-myc*-His6x tags; gray, the hinge and Fc domains of mouse IgG2c. (**B**) SDS–polyacrylamide gel electrophoresis analysis of purified monomeric nanobodies (lane 1), dimeric nanobodies (lane 2), HLE-dimeric nanobodies (lane 3), and reconstructed bivalent heavy chain antibodies (Nb-Fc) (lane 4). M, molecular weight marker proteins. (**C**) Potencies of monovalent and bivalent nanobodies to block (13A7) or enhance (14D5) ATP-induced ectodomain shedding of CD62L by Yac-1 cells. ATP was used at concentrations 2.5-fold above (13A7) and 2-fold below (14D5) the EC_{50} (50 μM) for the activation of P2X7 in Yac-1 cells. An irrelevant Nb-Fc fusion protein was used as a control. (**D**) IC_{50}/EC_{50} values for the blocking/potentiation of ATP-induced shedding of CD62L were calculated from the data in (C). (**E**) Potencies of bivalent nanobody 13A7-Fc and conventional monoclonal antibodies to block ATP-induced ectodomain shedding of CD62L by primary splenic T cells. Data are representative of two (E) or three (C and D) independent experiments.

Bivalent nanobodies modulate P2X7 function on primary mouse macrophages and T cells

Pore formation, inflammasome assembly, activation of caspase-1, and release of IL-1β are hallmarks of ATP-induced activation of P2X7 on macrophages, whereas ectodomain shedding and cell death are hallmarks of P2X7 activation on T cells. Treatment of mouse peritoneal macrophages with dimeric nanobodies effectively blocked (13A7) or potentiated (14D5) ATP-induced pore formation (fig. S3A), inflammasome assembly (fig. S3B), caspase-1–mediated cleavage of pro–IL-1β (fig. S3C), and release of IL-1β (fig. S3D), but it did not affect P2X7-independent inflammasome assembly in response to the K^+ ionophore nigericin (fig. S3B). Dimeric nanobodies 13A7 and 14D5 also did not affect transcription of *Il6* or *Il1b* genes in response to P2X7-independent activation of nuclear factor κB by LPS (fig. S3E). Treatment of primary T cells with dimeric nanobodies effectively blocked (13A7) or potentiated (14D5) ATP-induced shedding of CD27 (fig. S4A) and NAD-induced cell death (fig. S4B). In contrast, these nanobodies did not affect P2X7-independent proliferation of T cells in response to CD3–cross-linking antibodies (fig. S4C), confirming that the nanobodies act exclusively on P2X7-dependent cellular functions.

Nanobody 13A7-HLE blocks P2X7 in vivo in mice and ameliorates allergic contact dermatitis

To assess the capacity of nanobody 13A7 to reach and block P2X7 function on immune cells in vivo, we intravenously injected half-life–extended dimeric 13A7-HLE into the mice. Splenic T cells

and peritoneal macrophages were recovered at different time points after nanobody injection and were challenged ex vivo with ATP to assess target occupancy and functional blockade. 13A7-HLE effectively blocked both ATP-induced shedding of CD27 by splenic T cells and ATP-induced nuclear DAPI (4′,6-diamidino-2-phenylindole) uptake by peritoneal macrophages within 2 hours of nanobody injection (Fig. 4, A and B). Comparative analyses of dimeric (13A7-dimer) versus half-life–extended dimeric (13A7-HLE) nanobodies showed that fusion to the albumin-specific nanobody Alb8 resulted in a much longer blockade of P2X7 in vivo (Fig. 4C). Blockade of P2X7 by 13A7-HLE was still effective 96 hours after injection (Fig. 4B).

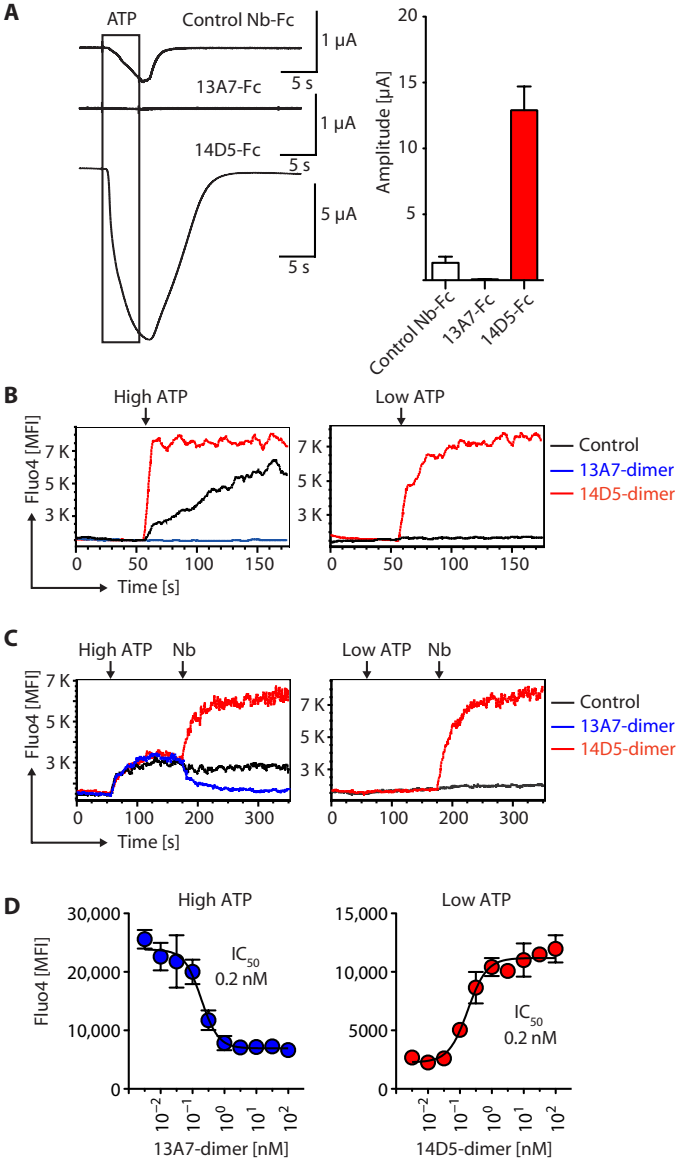

Fig. 3. Bivalent nanobodies block (13A7) or potentiate (14D5) the ion channel activity of P2X7. (**A**) Voltage-clamp recordings of ATP-induced currents in mouse P2X7–expressing *Xenopus* oocytes. Oocytes were preincubated with bivalent nanobodies (100 nM) for 20 min at room temperature before application of ATP for 5 s. Representative ATP-evoked currents recorded from individual oocytes are shown. Columns show mean amplitudes of ATP currents (n = 7 to 8 oocytes for each condition). (**B** to **D**) Flow cytometric analyses of Ca^{2+} influx into P2X7-transfected HEK cells loaded with the Ca^{2+} indicator Fluo-4. (B) Cells preincubated with bivalent nanobodies (100 nM) were analyzed for 1 min before addition of ATP and were then further analyzed for 2 min. (C) Cells were analyzed for 1 min before addition of ATP. After further incubation for 3 min, bivalent nanobodies (1 µM) were added, and cells were further analyzed for 3 min. (D) Cells preincubated with bivalent nanobodies (100 nM) were analyzed 10 min after addition of ATP. Data are representative of two (A to C) or three (D) independent experiments. MFI, mean fluorescence intensity.

Next, we probed the therapeutic potential of 13A7-HLE in a mouse model of allergic contact dermatitis in response to the contact allergen 1-fluoro-2,4-dinitrobenzene (DNFB). In this model, mice are sensitized by epicutaneous application of DNFB to the shaved abdominal skin (day 0). When challenged 6 days later with DNFB on the ear skin (day 6), mice respond with a characteristic local inflammatory response that can be monitored by the ear swelling reaction and the release of inflammatory cytokines 24 hours after challenge. Mice deficient for P2X7 are resistant to contact hypersensitivity, because dendritic cells fail to produce IL-1β in response to the contact allergen in the sensitization phase (*8*). Therefore, 13A7-HLE was systemically administered on days 0, 3, and 6. Blocking P2X7 via 13A7-HLE ameliorated local inflammation, because animals treated with nanobody 13A7-HLE had a significantly lower gain in ear weight than did control animals and significantly lower levels of the inflammatory cytokines IL-6 and IL-1β in ear tissue extracts (Fig. 4D). The therapeutic effect also required application of nanobodies during the challenge phase, because a single injection of 13A7-HLE before sensitization with DNFB did not significantly decrease inflammation (Fig. 4D). This suggests that P2X7 plays a role during both the sensitization and challenge phases of the inflammatory response, consistent with the finding that application of the contact allergen to the ear causes local release of ATP (*8*).

Nanobody 13A7-HLE ameliorates experimental glomerulonephritis in mice

To further assess the therapeutic potential of nanobody 13A7-HLE in inflammatory diseases, we analyzed its effects in a mouse model of experimental glomerulonephritis induced by injection of antibodies against glomerular podocytes (*33*). Before injection and every 3 days after injection of antipodocyte antibodies, we treated groups of mice with either 13A7-HLE, a control nanobody-HLE, or the P2X7-potentiating nanobody 14D5-HLE. We monitored disease progression using markers of renal function and acute inflammation, as well as by histological analyses of kidney sections. All animals receiving antipodocyte antibodies had deposits of immunoglobulin and complement component 3 along the basement membrane of glomerular capillaries (fig. S5). Animals treated with 13A7-HLE showed little, if any, inflammation; animals treated with 14D5-HLE had enhanced inflammation and kidney damage (Fig. 5). Albuminuria was significantly reduced after 15 days in animals treated with 13A7-HLE compared to animals treated with control nanobody-HLE (Fig. 5, A and B). Nanobody 13A7-HLE prevented the development of nephrotic syndrome, maintaining normal levels of blood urea nitrogen, serum triglycerides, and serum cholesterol (Fig. 5D), as well as preventing a rise of the proinflammatory cytokine IL-6 in serum and MCP-1 [monocyte chemoattractant protein-1 (*MCP-1*/CCL2)] in urine (Fig. 5D). Nanobody 13A7-HLE also inhibited histopathological signs of kidney damage, including tubular protein casts, glomerular capillary occlusion, swelling of podocytes, and disrupted nephrin staining at the filtration barrier (Fig. 5E). Immunohistochemical analyses of inflammatory cells revealed significantly reduced infiltration of $Ly6G^+$ granulocytes and $CD3^+$ T cells in the glomeruli of animals treated with 13A7-HLE compared to animals treated with control nanobody-HLE (Fig. 5F). Conversely, animals treated with 14D5-HLE

showed enhanced glomerular infiltration of granulocytes and T cells (Fig. 5G) and enhanced albuminuria (Fig. 5, A and B). Nanobody 14D5-HLE did not cause any significant effects on disease progression in *P2x7*$^{-/-}$ animals, confirming that the aggravating effect of this nanobody is mediated via P2X7 (Fig. 5C). Together, these data demonstrate that the P2X7-antagonizing nanobody 13A7-HLE ameliorates inflammation in two distinct disease models.

Human P2X7–specific nanobody Dano1 blocks IL-1β release from endotoxin-exposed human monocytes

Using human P2X7–expressing HEK cells for panning of phage display libraries, we selected a nanobody, designated Dano1, that recognizes human P2X7 with high specificity. Dano1 does not cross-react with mouse P2X7 or with human P2X1 or P2X4, the closest orthologs of P2X7 (Fig. 6A). Dano1 blocked ATP-induced Ca^{2+} influx and pore formation in these cells (Fig. 6B), and dimerization reduced the IC_{50} of Dano1 for ATP-induced Ca^{2+} influx and pore formation by HEK cells from 0.5 to 0.2 nM (Fig. 6C). Compared to the previously described human P2X7–antagonistic conventional monoclonal antibody (mAb) L4 (*32*), Dano1 demonstrated both higher potency (20- to 50-fold lower IC_{50}) and efficacy (>95% versus 60 to 70% maximal inhibition) (Fig. 6, B and C).

Dano1 blocked ATP-induced inflammasome assembly by LPS-primed human monocytes (Fig. 7A) but affected neither P2X7-independent

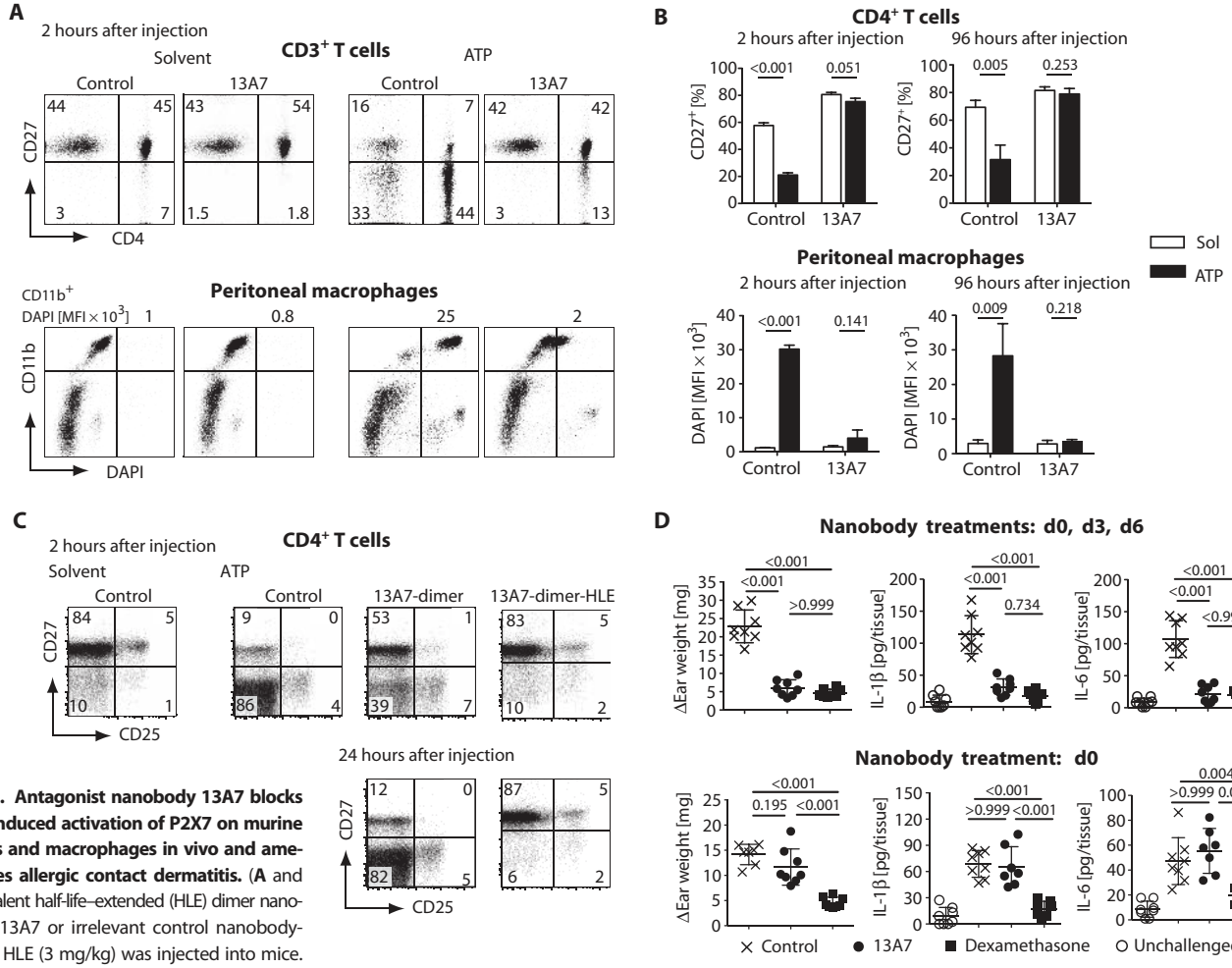

Fig. 4. Antagonist nanobody 13A7 blocks ATP-induced activation of P2X7 on murine T cells and macrophages in vivo and ameliorates allergic contact dermatitis. (**A** and **B**) Bivalent half-life–extended (HLE) dimer nanobody 13A7 or irrelevant control nanobody-dimer HLE (3 mg/kg) was injected into mice. Splenocytes and peritoneal macrophages were prepared 2 or 96 hours after injection. Ectodomain shedding of CD27 was monitored by flow cytometry on primary spleen cells treated for 20 min with solvent (Sol) or ATP in the presence of HLE-nanobodies. Gating was performed on $CD3^+$ T cells. DAPI uptake was monitored on primary peritoneal macrophages treated for 20 min with solvent or ATP in the presence of HLE-nanobodies. Numbers in the upper panels indicate the percentage of cells in the respective quadrants; numbers on top of the lower panels indicate the DAPI MFI of $CD11b^+$ cells. (B) $CD27^+$ cells (percentage of $CD4^+$ cells) (top) and DAPI MFI ± SD (bottom) were quantified from flow data as in (A) (n = 3 to 5 mice). P values were determined by Student's t test. (**C**) Splenocytes were prepared 2 hours (top) and 24 hours (bottom) after systemic injection of 13A7-dimer (2 mg/kg), 13A7-dimer HLE (3 mg/kg), or control nanobody-dimer HLE. Cells were incubated for 20 min in the presence of solvent or ATP before costaining with antibodies against CD4, CD25, and CD27. Gating was performed on $CD4^+$ T cells. (**D**) Mice were sensitized by the application of DNFB on the abdominal skin and challenged 6 days later by the application of DNFB on the left ear. Groups of mice (n = 8) were treated with 13A7-dimer HLE or control nanobody-dimer HLE (3 mg/kg) on day 0 (d0) (2 hours before sensitization) (top and bottom). Mice indicated in the upper panels received additional nanobody injections on days 3 and 6 (2 hours before challenge). A control group was treated with dexamethasone 2 hours before challenge. Twenty-four hours after challenge, inflammation was scored as the difference in weight between the left and right ears. Inflammatory cytokines in ear tissue were quantified by enzyme-linked immunosorbent assay (ELISA). Data are from individual animals (n = 8), with means and SD indicated by bars and vertical lines. P values were determined by one-way analysis of variance (ANOVA), followed by Bonferroni posttest. Data are representative of two (B and C), three (D, top), and one (D, bottom) independent experiments.

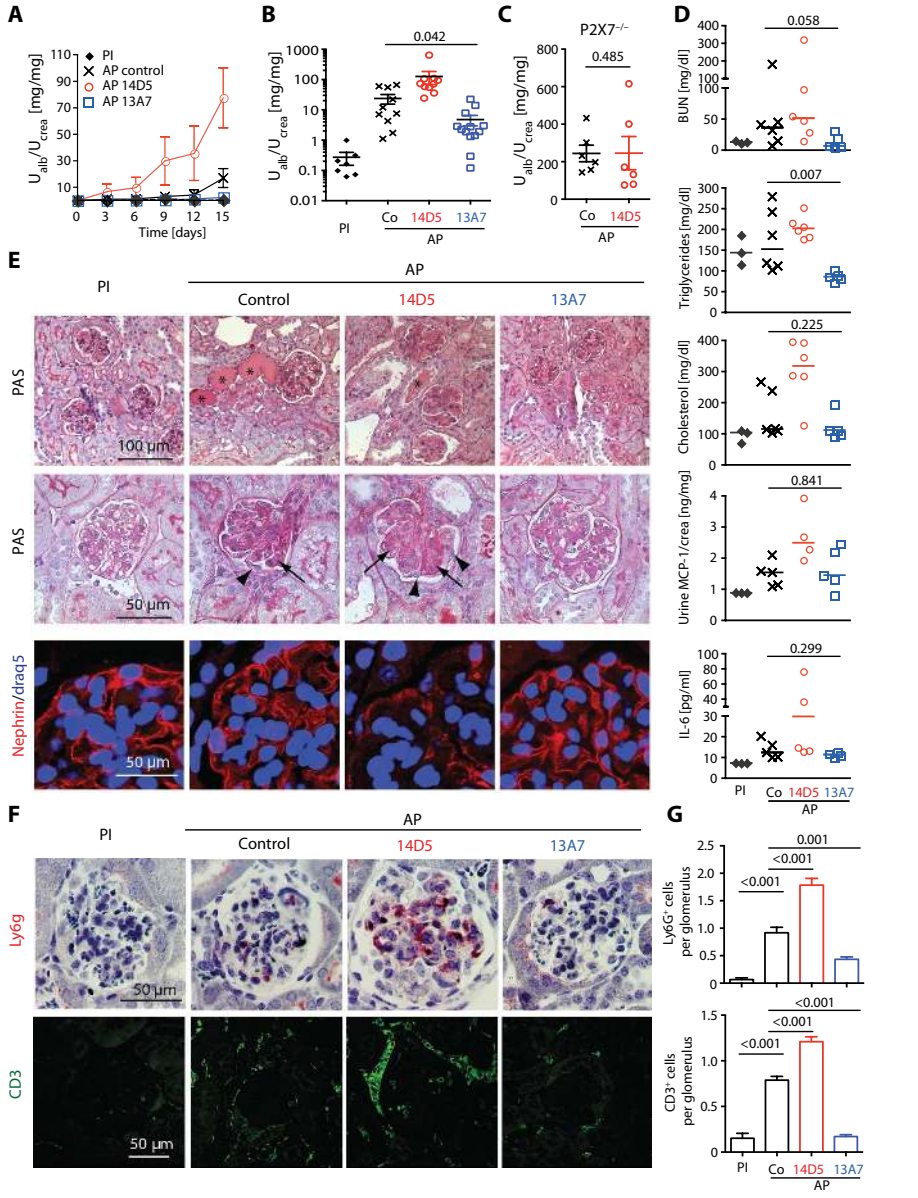

Fig. 5. P2X7-specific antagonist or potentiator nanobodies ameliorate (13A7) or worsen (14D5) inflammation in antipodocyte induced glomerulonephritis. (**A** to **G**) Glomerulonephritis was induced by injection of antipodocyte (AP) serum. Control mice received preimmune serum (PI). P2X7$^{-/-}$ animals were used in one control experiment (C), and wild-type mice were used in all other experiments. Groups of mice (n = 6 to 10) were treated with P2X7-specific 13A7-dimer HLE or 14D5-dimer HLE or control nanobody-dimer HLE (2 mg/kg) 2 hours before serum injection and additionally every 3 days (1 mg/kg). Urine albumin levels (U_{alb}) were quantified by ELISA, and urine creatinine levels (U_{crea}) were determined by automated measurement (A to C). Data in (A) show means ± SEM from n = 6 to 8 animals. Data in (B) and (C) are from individual animals (n = 8 to 16), with means and SEM indicated by bars and vertical lines. On the day of killing, blood urea nitrogen (BUN), serum triglycerides, and serum cholesterol levels were determined by automated measurement; IL-6 in serum and MCP-1 in urine were quantified by ELISA (D). Data in (B) to (D) are endpoint values on day 15. P values were determined by Mann-Whitney U test (n = 6 to 13). (E) Kidney sections were stained with periodic acid–Schiff. Tubular protein casts are marked by asterisks, and glomerular capillary occlusions and swollen podocytes are marked by arrows and arrowheads, respectively. Sections were also stained with the DNA staining dye draq5 and with antibodies against nephrin, a podocyte cell surface protein essential for the proper functioning of the renal filtration barrier (bottom). (F and G) Granulocytes and T cells in kidney sections were stained with antibodies against Ly6G and CD3, respectively, and infiltrating cells in glomeruli were quantified. Data are number of Ly6G$^+$ and of CD3$^+$ cells per glomerulus (n = 100 glomeruli from 10 to 13 mice in each group). Data are means ± SEM. P values were determined by Mann-Whitney U test. Data are representative of one (C and D), two (A), and three (B and E to G) independent experiments. Results in (B) and (G) show the cumulative data of two experiments with comparable endpoint values.

inflammasome assembly induced by nigericin (Fig. 7A) nor P2X7-independent transcription of *IL6* or *IL1B* in response to LPS (Fig. 7B). Similarly, Dano1 effectively blocked ATP-induced shedding of CD62L and the externalization of phosphatidylserine by human T cells (Fig. 7C) but did not affect P2X7-independent proliferation of T cells in response to anti-CD3 antibodies (Fig. 7D).

The critical role of P2X7 in release of the proinflammatory cytokine IL-1β underscores its importance as a therapeutic target in inflammation. To evaluate the potential therapeutic benefit of Dano1, we used a surrogate P2X7-mediated inflammation model and measured the release of IL-1β from monocytes in fresh human blood treated with LPS and ATP. Cells of all four healthy volunteer donors responded to this treatment with heightened secretion of IL-1β (Fig. 7, E and F). Dano1 blocked ATP-induced release of IL-1β with subnanomolar IC_{50} (Fig. 7E). Dano1 demonstrated up to 1000-fold higher potency than the small-molecule inhibitors of P2X7 currently in preclinical development for neurological and inflammatory diseases [JNJ47065567 (neurological diseases; Janssen) and AZ10606120 (renal injury; AstraZeneca)] (*15*, *16*). Its high specificity and potency make Dano1 an excellent clinical candidate.

DISCUSSION

Our study describes highly potent nanobody antagonists of the mouse and human P2X7 ion channel with higher specificity, better pharmacodynamics, and lower toxicity than current small-molecule antagonists. These nanobodies represent the first effective biologic antagonists of this emerging drug target for inflammatory disease (*15*, *18*). In two different experimental mouse models of inflammatory diseases, antibody-induced glomerulonephritis and allergic contact dermatitis, systemic injections of the half-life–extended antagonist nanobody 13A7 ameliorated disease. In a surrogate inflammation model with endotoxin-exposed fresh human blood samples, the nanobody Dano1 blocked the release of the proinflammatory cytokine IL-1β with up to 1000-fold higher potency than small-molecule inhibitors of P2X7 currently in development for inflammatory and neurological diseases (*15*, *18*).

In contrast to small molecules, biologics exhibit high specificity and have few off-target effects. The duration of nanobody-mediated blockade of P2X7 in vivo could easily be tailored: although dimeric nanobodies blocked P2X7 in vivo for several hours, fusion to the antialbumin nanobody Alb8 provided long-term in vivo blockade of P2X7 for at least 4 days, reflecting the serum half-life of mouse albumin of ca. 2 days. Hence, the presence of the clinically validated albumin-binding module provides the nanobodies with good pharmacokinetics and pharmacodynamic properties in vivo and allows the translation from mouse models and non-human primates to man (*34*). Clinical leads containing an albumin-binding module such as the anti-IL-6R nanobody ALX-0061 are being given every 2 to 4 weeks by subcutaneous injection for systemic lupus erythematosus and rheumatoid arthritis (NCT02437890 and NCT02287922).

Nanobody Dano1 is applicable for the treatment of systemic human inflammatory disorders in which high levels of ATP and IL-1β are found, including glomerulonephritis, lupus nephritis, and acute dermatitis. Previous pharmacological and genetic studies have already implicated P2X7 as a potential therapeutic target in glomerulonephritis, and an increase in glomerular expression of P2X7 was observed in renal biopsies from lupus nephritis patients, as well as in rat and mouse glomerulonephritis models (*1*, *7*). Taylor *et al.* showed that rats treated with a small-molecule P2X7 antagonist as well as P2X7-deficient mice display attenuated inflammatory kidney damage in response to the injection of antibodies against the glomerular basement membrane (*7*). Our results corroborate the therapeutic potential of P2X7 antagonistic nanobodies in this indication, because 13A7-HLE inhibited renal immune cell infiltration and P2X7-dependent kidney pathology. Moreover, the finding that the P2X7-enhancing nanobody 14D5-HLE aggravated glomerular inflammation substantiates the pathological role of P2X7 in this disease. It should be noted that the P2X7 nanobodies have been administrated from the onset of inflammation because the mouse model progresses more rapidly and aggressively than the human disease, in which the nanobodies would be applied in a therapeutical setting, after disease was established. In the acute dermatitis inflammatory response, P2X7 evidently plays a role during both the sensitization and challenge phases, consistent with the finding that application of the contact allergen to the ear causes local release of ATP (*8*). During the sensitization phase, P2X7 expression on dendritic cells is important for the activation of T cells (*8*). Nanobody 13A7-HLE effectively prevented local inflammation and effectively blocked release of proinflammatory IL-6 and IL-1β when present during the challenge phase, suggesting that multiple P2X7-expressing immune subsets are involved. Both disease indications hence seem valid options for the application of P2X7 antagonist nanobodies.

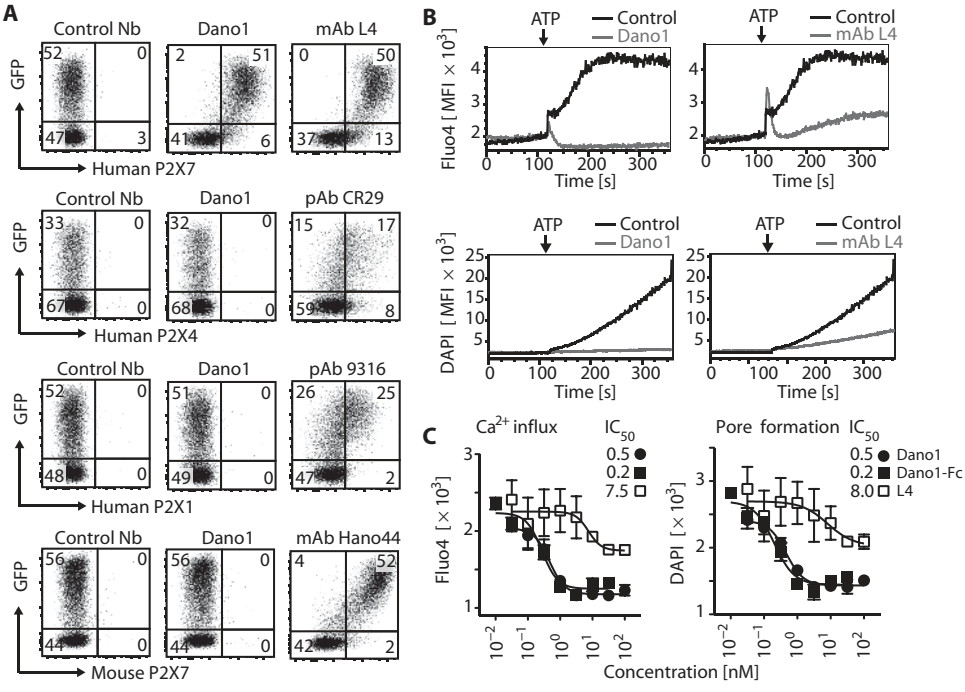

Fig. 6. Characterization of a nanobody Dano1 as a highly specific and potent antagonist of human P2X7. (**A**) Flow cytometric analyses illustrating the specificity of Dano1 using HEK293 T cells transiently cotransfected with GFP and human P2X7, human P2X4, human P2X1, or mouse P2X7. Twenty-four hours after transfection, cells were stained with Dano1-Fc or an irrelevant Nb-Fc. Control staining was performed with the indicated conventional antibodies directed against P2X1, P2X4, or P2X7. pAb, polyclonal antibody. (**B**) Flow cytometric analyses illustrating the capacity of nanobody Dano1 to block ATP-induced Ca^{2+} influx (top) and uptake of DAPI (bottom) by HEK293 cells stably transfected with human P2X7. Cells loaded with the Ca^{2+} indicator Fluo-4 were preincubated with Dano1-Fc or mAb L4 and adjusted to 37°C in a water bath for 2 min before flow cytometry. After addition of ATP and DAPI, cells were analyzed for 4 min further. Gating of the ion channel was assessed by changes in the MFI of Fluo-4. Pore formation was assessed by the changes in the MFI of DAPI. (**C**) HEK293 stably transfected with human P2X7 were loaded with Fluo-4 and incubated for 20 min with ATP in the presence of DAPI and serial dilutions of monomeric Dano1, bivalent Dano1-Fc, or mAb L4 before fluorimetry. (A to C) Data are representative of three independent experiments.

In addition, inflammatory bowel disease is a potential indication, because P2X7 and IL-1β participate in both initiation and regulation of intestinal inflammation (*21*, *30*). P2X7 is differentially expressed in the mucosa of patients with active and quiescent inflammatory bowel disease. An increase in the number of colonic mast cells expressing P2X7 has been observed in patients with Crohn's disease and in a mouse model of experimentally induced colitis. In the latter, treatment with a mouse P2X7–specific antibody inhibited mast cell activation and intestinal inflammation (*30*). Moreover, the small-molecule inhibitor of P2X7 AZD9056 showed improved clinical parameters in a phase 2 study in patients with moderate-to-severe Crohn's disease, although there was a lack of objective change in the biomarkers of inflammation (*21*). It seems that AZD9056 modulated pain rather than the chronic inflammatory response in this setting, consistent with the evidence for a role of P2X7 in chronic pain (*4*, *5*).

Llama immunization also yielded another P2X7 nanobody, 14D5, that reduced the ATP threshold required for gating of mouse P2X7. In comparison to other P2X receptors, gating of P2X7 requires relatively high concentrations of ATP (*35*). It is unknown whether such high concentrations can be achieved in extracellular compartments other than the immediate vicinity of necrotic cells.

However, a number of substances including LL37, polymyxin B, and ivermectin potentiate gating of P2X7 in an allosteric manner (*36*, *37*). It is conceivable that 14D5 similarly allosterically facilitates the conformational change required for gating of P2X7. Systemic injections of 14D5-HLE aggravated disease parameters in the glomerulonephritis model. Although such proinflammatory effects would be undesired in a chronic inflammatory disease, enhancing P2X7-mediated inflammation might be therapeutically useful in other pathophysiological situations, for instance, in cancer or infections with intracellular parasites.

The usefulness of nanobodies as specific modulators of P2X7 function in the clinic may be limited by three factors. First, common allelic variants affect the sensitivity of P2X7 to extracellular ATP (*38*, *39*). P2X7 antagonist nanobodies could be more effective in patients expressing highly sensitive P2X7 variants. Although we have verified Dano1 efficacy in human immune cells from several donors, a full genotype analysis would be advisable before commencing clinical trials. Second, nanobodies have a low intrinsic propensity to cross the blood-brain barrier, similar to conventional antibodies, which restricts brain uptake and application to neurological disorders. For inflammatory diseases of the central nervous system, it may be necessary to engineer P2X7 antagonist nanobodies for improved crossing of the blood-brain barrier (*29*, *40*). Third, the development of antibodies to a nanobody in a patient is a potential limitation of any biologic. Although nanobodies have a high intrinsic sequence identity to human germ line V_H (variable region of immunoglobulin heavy chain), lead candidates are further sequence-optimized for even lower immunogenicity (*41*). The level of treatment-related antibodies toward nanobodies that have been tested in clinical trails is in the same range as that for marketed human and humanized antibodies (*42*).

Numerous examples of nanobodies in successful clinical development now exist, with eight different nanobodies currently in clinical trials, the most advanced being in phase 3 for thrombotic thrombocytopenic purpura (NCT02553317). Efficacy of nanobodies in inflammatory disease has been demonstrated in multiple clinical trials, including phase 2 trials of vobariluzumab directed against the IL-6 receptor for rheumatoid arthritis (*34*) and of caplacizumab directed against von Willebrand factor for acquired thrombotic thrombocytopenic purpura (NCT01284569 and NCT01020383) (*42*). Our P2X7 antagonist nanobodies would likely follow a similar translational path to the clinic, after the successful assessment of the pharmacological and pharmacodynamic parameters and safety profile in preclinical species.

The nanobodies described here may represent the next generation of highly specific, long-acting P2X7 antagonist

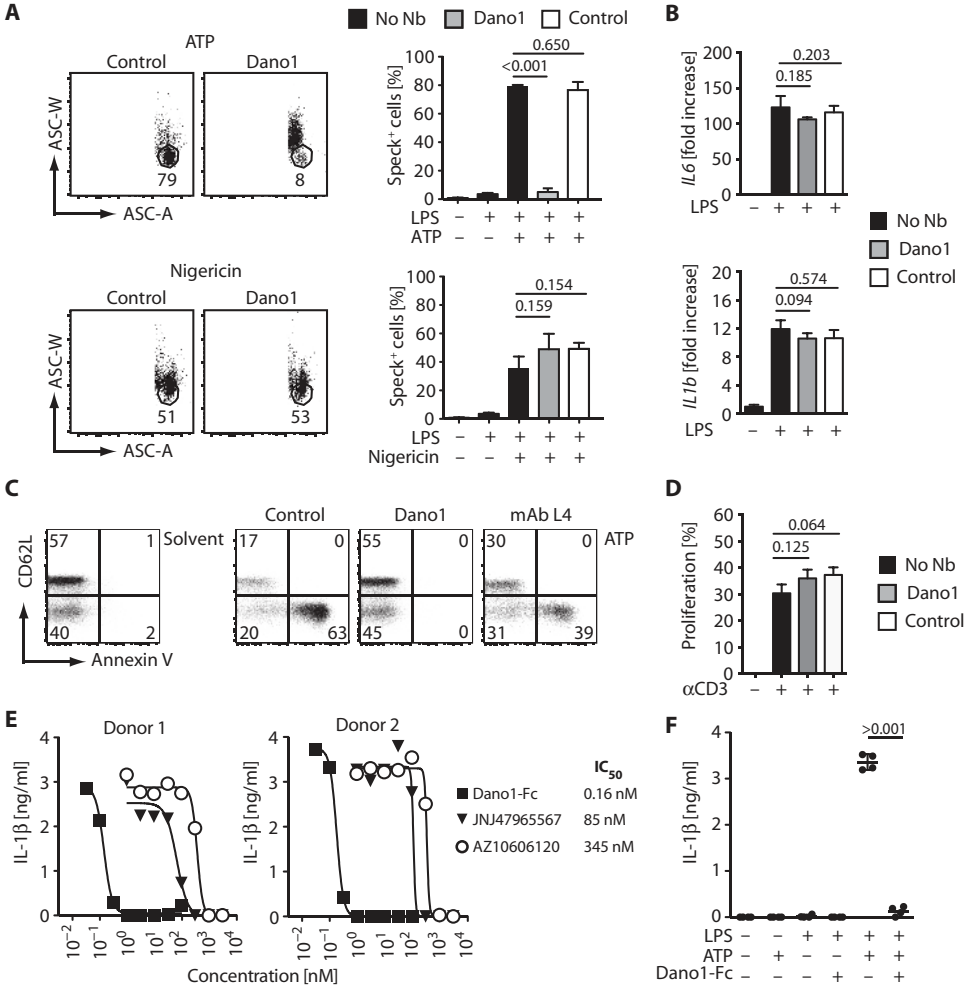

Fig. 7. Antagonist nanobody Dano1 blocks ATP-induced activation of P2X7 in primary human monocytes and T cells as well as ATP-induced release of IL-1β in endotoxin-exposed blood. (**A**) Inflammasome assembly was monitored on human blood monocytes by flow cytometry using an antibody directed against the adaptor protein ASC. Cells were treated for 2 hours with LPS and then further incubated for 30 min with ATP (top) or nigericin (bottom) in the absence or presence of Dano1-Fc or control Nb-Fc (200 nM). Data shown in column diagrams are percentage of speck$^+$ cells ± SD calculated from flow data (n = 3 donors). P values were determined by one-way ANOVA, followed by Bonferroni posttest. (**B**) P2X7-independent activation of NF-κB–mediated transcription of *IL6* and *IL1B* in purified human blood monocytes was monitored by quantitative reverse transcription PCR (qRT-PCR), after treatment of cells for 3 hours with LPS in the absence or presence of Dano1-Fc or control Nb-Fc (200 nM). Data show the fold increase in gene transcription ± SD (n = 4). P values were determined by one-way ANOVA, followed by Bonferroni posttest. (**C**) Ectodomain shedding of CD62L and externalization of phosphatidylserine were monitored by flow cytometry on primary human T cells treated for 20 min with solvent or ATP in the presence of Dano1-Fc, control Nb-Fc, or mAb L4. Gating was performed on CD4$^+$ T cells. Numbers indicate percentage of cells in the respective quadrants. (**D**) Proliferation of human T cells in response to treatment with anti-CD3 was monitored by flow cytometric analysis of eFluor dye dilution after incubation of cells for 4 days in the absence or presence of half-life–extended nanobodies. Gating was performed on living CD4$^+$ cells. Data show percentage of proliferating cells ± SD (n = 3). P values were determined by one-way ANOVA, followed by Bonferroni posttest. (**E** and **F**) IL-1β levels were monitored by ELISA after sequential treatment of blood samples with LPS for 1.5 hours and with ATP for 0.5 hour. Samples were treated in the presence of serial dilutions of Dano1-Fc or the small-molecule antagonists in clinical development (JNJ47965567 or AZ10606120) (E) or with 100 nM Dano1-Fc (F). P values were determined by Student's t test (n = 4 donors). Data are representative of two (B, D, and E), three (A and C), or four (F) independent experiments.

drugs. Given the central role of IL-1β in chronic inflammatory diseases, antagonizing P2X7 may be an attractive alternative or complementary strategy to blocking IL-1β. The modular nature of the nanobody technology allows the combination of nanobody modules with different specificities. Similarly, fusion to nanobodies that bind lineage-specific cell surface proteins may allow targeting of P2X7-specific nanobodies to specific cell types, such as regulatory T cells or inflammatory monocytes. In general, the strategy described here—llama immunization combined with nanobody development—may be useful for generating specific functional biologics against other leukocyte ion channels that are promising drug targets.

MATERIALS AND METHODS

Study design

Our study was designed to determine whether activation of the P2X7 ion channel can be inhibited in vitro and in vivo with anti-P2X7 nanobodies. We derived 19 new anti-P2X7 nanobodies. We identified one nanobody (13A7) that inhibits ATP-induced gating of mouse P2X7 and one nanobody (14D5) that potentiates ATP-induced gating of mouse P2X7 and one nanobody (Dano1) that inhibits ATP-induced gating of human P2X7. We used established preclinical inflammatory models to evaluate the inhibitory activity of mouse P2X7–specific nanobody 13A7 in vivo. Previous studies had demonstrated that disease in these models can be ameliorated by broad-spectrum P2X7 antagonists (*7*, *8*). In the mouse model of allergic contact dermatitis [delayed type hypersensitivity (DTH) model], an ear-swelling response is induced by painting the allergen DNFB onto the abdominal skin ("sensitization"), followed 6 days later by a second application of the allergen onto one ear ("challenge"). In the mouse model of glomerulonephritis (GN model), an inflammatory response is induced by injection of sheep anti-mouse podocyte antibodies, resulting in the deposition of antibodies and complement components along glomerular capillaries. The inflammatory response in the DTH model can be quantified conveniently 24 hours after the challenge by the gain in ear weight and the local release of the inflammatory cytokines IL-1β and IL-6. In the GN model, the loss of albumin to the urine serves as an indicator of damage to the glomerular filtration barrier and the appearance of neutrophils and T cells in glomeruli as an indicator of the local inflammatory response. To ensure a sustained blockade of P2X7 throughout the course of these aggressive disease models, we injected half-life–extended dimeric nanobodies 2 hours before induction of disease and, again, every 3 days after induction of disease. Dosage and timing of nanobody administration were determined by pharmacodynamic simulation studies aiming to maintain a serum concentration of 100 nM for the half-life–extended nanobodies (100-fold above the IC_{50}), on the basis of previously determined in vivo half-life for HLE-dimeric nanobodies of 1.3 to 1.9 days. Animals were killed after 7 days (DTH model) or 15 days (GN model), that is, at the expected peak of the respective inflammatory responses.

To evaluate the inhibitory activity of the human P2X7–specific nanobody Dano1 in vivo, we used a surrogate inflammation model in which fresh samples of human blood were treated sequentially with endotoxin (LPS) and ATP. This induces a massive, P2X7-dependent release of IL-1β, providing a means to test the therapeutic potential of Dano1 in inflammation. Mice were assigned randomly to experimental groups. The sample size was determined by power analyses. Studies were blinded. Numbers of replicates are indicated in the figures or in the corresponding legends for all experiments.

Selection and characterization of P2X7-specific Nanobodies

Phage libraries were selected in suspension on Chinese hamster ovary cells transfected with mouse P2X7. Bound phages were eluted by trypsinization, amplified in TG1 *Escherichia coli*, and reselected on Yac-1 cells endogenously expressing mouse P2X7. Single colonies were picked for screening of monovalent nanobodies by phage ELISA on fixed cells, after which positive hits were sequenced. For each unique sequence, protein expression was induced with isopropyl-β-D-thiogalactopyranoside for 3 hours during exponential growth. Periplasmic lysates were generated by osmotic shock and removal of bacterial debris by high-speed centrifugation. Nanobodies in crude periplasmic extracts were screened for selective binding to P2X7-transfected HEK cells by flow cytometry, either directly or after preincubation of extracts with fluorescein isothiocyanate–labeled anti–c-*myc* mAb (clone 9E10) for 30 min to form nanobody–anti-tag mAb complexes.

Multivalent formatting of Nanobodies

Homodimeric bivalent nanobodies were constructed by PCR using a 35-GS linker $(GGGGS)_7$ to fuse the two nanobodies. Half-life–extended nanobody formats were constructed using PCR by fusing the homodimeric nanobody via a 9-GS linker (GGGGSGGGG) to a third nanobody, Alb8, an albumin-specific nanobody (*28*). The Nb-Fc fusion format was generated by subcloning the VHH coding sequence upstream of the hinge and Fc domains of mouse IgG2c in the pCSE2.5 eukaryotic expression vector (provided by T. Schirrmann, Technical University Braunschweig, Germany) (*43*). Monovalent, bivalent, and HLE nanobodies were expressed as c-*myc*-His6x–tagged proteins in either *E. coli*, *Pichia pastoris* strain X-33, or HEK-6E cells (*44*) and purified by immobilized metal affinity chromatography using Ni–nitrilotriacetic acid beads (*45*). Fc fusion proteins were expressed in HEK-6E cells and purified by affinity chromatography using protein G–Sepharose (GE Healthcare).

Ectodomain shedding and cell death by Yac-1 cells and murine and human T cells

Anti-CD3 (145-2C11), anti-CD4 (RM4-5 and RPA-T4), anti-CD8 (RPA-T8), anti-CD25 (PC61), and anti-CD62L (MEL-14 and DREG-56) were obtained from BD; anti-CD27 (LG.3A10) was from BioLegend. Cells were preincubated with P2X7-specific or control nanobodies for 15 min at 4°C and then further incubated for 20 min at 37°C in RPMI medium in the absence or presence of ATP (*46*, *47*). Cells were washed, stained with fluorochrome-conjugated antibodies, and analyzed by flow cytometry (FACSCanto II, BD; and FlowJo software, Tree Star). For cell death analyses, T cells were stained with fluorochrome-conjugated annexin V (BD) and antibodies in annexin V–binding buffer for 20 min, washed, and analyzed by flow cytometry in the presence of propidium iodide (Sigma).

T cell proliferation assays

Mouse CD4 T cells were purified from spleen and peripheral lymph nodes by negative selection using magnetic beads (Miltenyi). Cells were labeled with 2 μM carboxyfluorescein succinimidyl ester (CFSE; Invitrogen) for 30 min at 37°C. Cells were washed and preincubated in complete RPMI medium (supplemented with 10% fetal calf serum, L-glutamine, pennicilin, and streptomycin; all from Gibco) in the absence or presence of nanobodies for 20 min before seeding onto a 24-well plate coated with anti-CD3 and anti-CD28 (each at 1 μg per well; BD) at 5×10^5 cells per well. Proliferation of T cells was analyzed after 3 days by CFSE dilution by flow cytometry. Human peripheral blood

mononuclear cells were labeled with 2 μM eFluor 670 (eBioscience) for 10 min at 37°C. Cells were washed and resuspended in complete RPMI medium in the absence or presence of anti-CD3 (400 ng/ml; OKT3, BioLegend). Cells were seeded onto a round-bottom 96-well plate at 80,000 cells per well in the absence or presence of nanobodies at a final concentration of 100 nM. Nanobodies were added a second time after 2 days of culture. After 4 days, cells were stained with anti-CD4 (RPA-T4) and anti-CD8 (SK1), and proliferation of living T cells was analyzed by eFluor dye dilution by flow cytometry.

Experimentally induced allergic contact dermatitis

Three groups (n = 8) of adult 9- to 10-week-old female C57BL/6J mice were sensitized by two applications in a 24-hour interval of DNFB (Aldrich) (30 μl of a 0.5% solution in acetone/olive oil, 4:1; Acros Organics) to the shaved abdominal skin. Two hours before the first application, two groups of mice received intraperitoneal injections of half-life–extended, Alb8-fusion proteins of nanobody 13A7 or a control nanobody [3 mg/kg in 200 μl of phosphate-buffered saline (PBS)]. These mice received one further intraperitoneal injection of the respective half-life–extended nanobodies on day 3 and an intravenous injection on day 6, 2 hours before challenge (both at a concentration of 3 mg/kg). The third group of mice received dexamethasone (200 μg/200 μl; Sigma) per os on day 6, 2 hours before challenge. Mice were challenged by the application of DNFB (20 μl of 0.2% solution in acetone/olive oil) to the right ear. As control, mice received applications of solvent (20 μl of acetone/olive oil, 4:1) to the left ear. Mice were killed 24 hours after challenge, and the disease course was monitored by measuring ear weight. The disease score is represented as the difference in ear weight of the right ear (treated with DNFB) and the left ear (treated with solvent). IL-6 and IL-1β in lysates of challenged und unchallenged ears were determined by ELISA. Allergic contact dermatitis experiments were performed by Washington Biotechnology Inc., Bethesda, MD.

Experimentally induced antipodocyte nephritis

Groups of C57BL/6J mice (n = 6 to 10) received intravenous injections of antipodocyte serum or preimmune serum (200 μl; concentrated twofold by centrifugation through centrifugal filters) (*33*), preceded by intravenous injections of half-life–extended nanobodies (2 mg/kg in 100 μl of saline). The mice received further intraperitoneal injections of half-life–extended nanobodies (1 mg/kg in 1 ml of saline) every 3 days. Urine was collected in metabolic cages for 4 to 6 hours after nanobody injection. Disease course was monitored by proteinuria using qualitative urine sticks. Mice were killed on day 15 or 21. Albumin and MCP-1 in urine and IL-6 in serum were quantified by sandwich ELISA (Bethyl, eBioscience) (*33*). Urine creatinine, blood urea nitrogen, serum triglycerides, and serum cholesterol were determined by an automated procedure in the central diagnostic laboratory of the University Medical Center Hamburg. For detection of T cells and granulocytes, 2-μm-thick paraffin sections obtained from kidneys fixed in 4% formalin were deparaffinized and rehydrated to water. Antigen retrieval was performed by digestion with protease XXIV (5 μg/ml; Sigma) for 15 min at 37°C (for Ly6G staining) or by boiling in citrate buffer (pH 6.1) for 30 min at 98°C (for CD3 staining). Unspecific binding was blocked by incubation with blocking buffer [5% normal horse serum (Vector) in PBS–0.05% Triton X-100] for 30 min at room temperature. Primary antibodies [rabbit anti-CD3 (1:1000; Dako) and rat anti-Ly6G (1:400; Hycult Biotech)] were incubated overnight at 4°C in blocking buffer. Visualization of staining was performed using the ZytoChem Plus AP Polymer Kit (Zytomed Systems) according to the manufacturer's instructions using neufuchsin (Merck). Nuclei were counterstained with hemalaun (Merck). $CD3^+$ and $Ly6G^+$ cells in glomeruli were quantified in 10 high-power visual fields (400×) per kidney in 6 to 10 mice per experimental group of n = 3 independent experiments. A visual field comprised one to three glomeruli.

Statistical analysis

Statistical analyses were performed with GraphPad Prism. Two groups were compared with Mann-Whitney U or Student's t test. Three or more groups were analyzed by one-way ANOVA, followed by Bonferroni posttests.

SUPPLEMENTARY MATERIALS

www.sciencetranslationalmedicine.org/cgi/content/full/8/366/366ra162/DC1
Materials and Methods
Fig. S1. Screening nanobodies for specific binding to P2X7.
Fig. S2. Pharmacological characterization of nanobodies 13A7 and 14D5.
Fig. S3. Bivalent nanobodies block (13A7) or potentiate (14D5) ATP-induced activation of P2X7 in primary mouse macrophages.
Fig. S4. Bivalent nanobodies block (13A7) or potentiate (14D5) nucleotide-induced activation of P2X7 in primary mouse T cells.
Fig. S5. Systemic injection of half-life–extended nanobodies ameliorates (13A7-HLE) or enhances (14D5-HLE) nephritis induced by antipodocyte antibodies.
Table S1. Anti-mouse P2X7 nanobodies selected from llamas immunized with P2X7-transfected HEK cells or with a P2X7 cDNA expression vector.
References (*48*–*50*)

REFERENCES AND NOTES

1. C. M. Turner, F. W. K. Tam, P.-C. Lai, R. M. Tarzi, G. Burnstock, C. D. Pusey, H. T. Cook, R. J. Unwin, Increased expression of the pro-apoptotic ATP-sensitive $P2X_7$ receptor in experimental and human glomerulonephritis. *Nephrol. Dial. Transplant.* **22**, 386–395 (2007).
2. O. Oyanguren-Desez, A. Rodríguez-Antigüedad, P. Villoslada, M. Domercq, E. Alberdi, C. Matute, Gain-of-function of P2X7 receptor gene variants in multiple sclerosis. *Cell Calcium* **50**, 468–472 (2011).
3. B. J. Gu, J. Field, S. Dutertre, A. Ou, T. J. Kilpatrick, J. Lechner-Scott, R. Scott, R. Lea, B. V. Taylor, J. Stankovich, H. Butzkueven, M. Gresle, S. M. Laws, S. Petrou, S. Hoffjan, D. A. Akkad, C. A. Graham, S. Hawkins, A. Glaser, S. K. Bedri, J. Hillert, C. Matute, A. Antiguedad; ANZgene Consortium, J. S. Wiley, A rare P2X7 variant Arg307Gln with absent pore formation function protects against neuroinflammation in multiple sclerosis. *Hum. Mol. Genet.* **24**, 5644–5654 (2015).
4. R. E. Sorge, T. Trang, R. Dorfman, S. B. Smith, S. Beggs, J. Ritchie, J.-S. Austin, D. V. Zaykin, H. Vander Meulen, M. Costigan, T. A. Herbert, M. Yarkoni-Abitbul, D. Tichauer, J. Livneh, E. Gershon, M. Zheng, K. Tan, S. L. John, G. D. Slade, J. Jordan, C. J. Woolf, G. Peltz, W. Maixner, L. Diatchenko, Z. Seltzer, M. W. Salter, J. S. Mogil, Genetically determined P2X7 receptor pore formation regulates variability in chronic pain sensitivity. *Nat. Med.* **18**, 595–599 (2012).
5. I. P. Chessell, J. P. Hatcher, C. Bountra, A. D. Michel, J. P. Hughes, P. Green, J. Egerton, M. Murfin, J. Richardson, W. L. Peck, C. B. Grahames, M. A. Casula, Y. Yiangou, R. Birch, P. Anand, G. N. Buell, Disruption of the P2X7 purinoceptor gene abolishes chronic inflammatory and neuropathic pain. *Pain* **114**, 386–396 (2005).
6. J. M. Labasi, N. Petrushova, C. Donovan, S. McCurdy, P. Lira, M. M. Payette, W. Brissette, J. R. Wicks, L. Audoly, C. A. Gabel, Absence of the $P2X_7$ receptor alters leukocyte function and attenuates an inflammatory response. *J. Immunol.* **168**, 6436–6445 (2002).
7. S. R. J. Taylor, C. M. Turner, J. I. Elliott, J. McDaid, R. Hewitt, J. Smith, M. C. Pickering, D. L. Whitehouse, H. T. Cook, G. Burnstock, C. D. Pusey, R. J. Unwin, F. W. K. Tam, $P2X_7$ deficiency attenuates renal injury in experimental glomerulonephritis. *J. Am. Soc. Nephrol.* **20**, 1275–1281 (2009).
8. F. C. Weber, P. R. Esser, T. Müller, J. Ganesan, P. Pellegatti, M. M. Simon, R. Zeiser, M. Idzko, T. Jakob, S. F. Martin, Lack of the purinergic receptor $P2X_7$ results in resistance to contact hypersensitivity. *J. Exp. Med.* **207**, 2609–2619 (2010).
9. D. Ferrari, C. Pizzirani, E. Adinolfi, R. M. Lemoli, A. Curti, M. Idzko, E. Panther, F. Di Virgilio, The $P2X_7$ receptor: A key player in IL-1 processing and release. *J. Immunol.* **176**, 3877–3883 (2006).

10. M. Idzko, D. Ferrari, H. K. Eltzschig, Nucleotide signalling during inflammation. *Nature* **509**, 310–317 (2014).
11. P. Pelegrin, A. Surprenant, Pannexin-1 mediates large pore formation and interleukin-1β release by the ATP-gated $P2X_7$ receptor. *EMBO J.* **25**, 5071–5082 (2006).
12. F. Scheuplein, N. Schwarz, S. Adriouch, C. Krebs, P. Bannas, B. Rissiek, M. Seman, F. Haag, F. Koch-Nolte, NAD^+ and ATP released from injured cells induce $P2X_7$-dependent shedding of CD62L and externalization of phosphatidylserine by murine T cells. *J. Immunol.* **182**, 2898–2908 (2009).
13. S. D. Guile, L. Alcaraz, T. N. Birkinshaw, K. C. Bowers, M. R. Ebden, M. Furber, M. J. Stocks, Antagonists of the $P2X_7$ receptor. From lead identification to drug development. *J. Med. Chem.* **52**, 3123–3141 (2009).
14. W. A. Carroll, D. Donnelly-Roberts, M. F. Jarvis, Selective $P2X_7$ receptor antagonists for chronic inflammation and pain. *Purinergic Signalling* **5**, 63–73 (2009).
15. R. Bartlett, L. Stokes, R. Sluyter, The P2X7 receptor channel: Recent developments and the use of P2X7 antagonists in models of disease. *Pharmacol. Rev.* **66**, 638–675 (2014).
16. C. C. Chrovian, J. C. Rech, A. Bhattacharya, M. A. Letavic, P2X7 antagonists as potential therapeutic agents for the treatment of CNS disorders. *Prog. Med. Chem.* **53**, 65–100 (2014).
17. N. Arulkumaran, R. J. Unwin, F. W. Tam, A potential therapeutic role for P2X7 receptor (P2X7R) antagonists in the treatment of inflammatory diseases. *Expert Opin. Invest. Drugs* **20**, 897–915 (2011).
18. A. Bhattacharya, K. Biber, The microglial ATP-gated ion channel P2X7 as a CNS drug target. *Glia* **64**, 1772–1787 (2016).
19. E. C. Keystone, M. M. Wang, M. Layton, S. Hollis, I. B. McInnes; D1520C00001 Study Team, Clinical evaluation of the efficacy of the $P2X_7$ purinergic receptor antagonist AZD9056 on the signs and symptoms of rheumatoid arthritis in patients with active disease despite treatment with methotrexate or sulphasalazine. *Ann. Rheum. Dis.* **71**, 1630–1635 (2012).
20. T. C. Stock, B. J. Bloom, N. Wei, S. Ishaq, W. Park, X. Wang, P. Gupta, C. A. Mebus, Efficacy and safety of CE-224,535, an antagonist of $P2X_7$ receptor, in treatment of patients with rheumatoid arthritis inadequately controlled by methotrexate. *J. Rheumatol.* **39**, 720–727 (2012).
21. A. Eser, J.-F. Colombel, P. Rutgeerts, S. Vermeire, H. Vogelsang, M. Braddock, T. Persson, W. Reinisch, Safety and efficacy of an oral inhibitor of the purinergic receptor $P2X_7$ in adult patients with moderately to severely active Crohn's disease: A randomized placebo-controlled, double-blind, phase IIa study. *Inflammatory Bowel Dis.* **21**, 2247–2253 (2015).
22. H. Sun, M. Li, Antibody therapeutics targeting ion channels: Are we there yet? *Acta Pharmacol. Sin.* **34**, 199–204 (2013).
23. Nanobody® is a trademark by Ablynx.
24. E. De Genst, K. Silence, K. Decanniere, K. Conrath, R. Loris, J. Kinne, S. Muyldermans, L. Wyns, Molecular basis for the preferential cleft recognition by dromedary heavy-chain antibodies. *Proc. Natl. Acad. Sci. U.S.A.* **103**, 4586–4591 (2006).
25. J. Wesolowski, V. Alzogaray, J. Reyelt, M. Unger, K. Juarez, M. Urrutia, A. Cauerhff, W. Danquah, B. Rissiek, F. Scheuplein, N. Schwarz, S. Adriouch, O. Boyer, M. Seman, A. Licea, D. V. Serreze, F. A. Goldbaum, F. Haag, F. Koch-Nolte, Single domain antibodies: Promising experimental and therapeutic tools in infection and immunity. *Med. Microbiol. Immunol.* **198**, 157–174 (2009).
26. F. Van Bockstaele, J. B. Holz, H. Revets, The development of nanobodies for therapeutic applications. *Curr. Opin. Invest. Drugs* **10**, 1212–1224 (2009).
27. S. Muyldermans, Nanobodies: Natural single-domain antibodies. *Annu. Rev. Biochem.* **82**, 775–797 (2013).
28. B. M. Tijink, T. Laeremans, M. Budde, M. Stigter-van Walsum, T. Dreier, H. J. de Haard, C. R. Leemans, G. A. van Dongen, Improved tumor targeting of anti–epidermal growth factor receptor Nanobodies through albumin binding: Taking advantage of modular Nanobody technology. *Mol. Cancer Ther.* **7**, 2288–2297 (2008).
29. G. K. Farrington, N. Caram-Salas, A. S. Haqqani, E. Brunette, J. Eldredge, B. Pepinsky, G. Antognetti, E. Baumann, W. Ding, E. Garber, S. Jiang, C. Delaney, E. Boileau, W. P. Sisk, D. B. Stanimirovic, A novel platform for engineering blood-brain barrier-crossing bispecific biologics. *FASEB J.* **28**, 4764–4778 (2014).
30. Y. Kurashima, T. Amiya, T. Nochi, K. Fujisawa, T. Haraguchi, H. Iba, H. Tsutsui, S. Sato, S. Nakajima, H. Iijima, M. Kubo, J. Kunisawa, H. Kiyono, Extracellular ATP mediates mast cell-dependent intestinal inflammation through P2X7 purinoceptors. *Nat. Commun.* **3**, 1034 (2012).
31. S. Möller, C. Jung, S. Adriouch, G. Dubberke, F. Seyfried, M. Seman, F. Haag, F. Koch-Nolte, Monitoring the expression of purinoceptors and nucleotide-metabolizing ecto-enzymes with antibodies directed against proteins in native conformation. *Purinergic Signalling* **3**, 359–366 (2007).
32. G. Buell, I. P. Chessell, A. D. Michel, G. Collo, M. Salazzo, S. Herren, D. Gretener, C. Grahames, R. Kaur, M. H. Kosco-Vilbois, P. P. A. Humphrey, Blockade of human $P2X_7$ receptor function with a monoclonal antibody. *Blood* **92**, 3521–3528 (1998).
33. C. Meyer-Schwesinger, S. Dehde, P. Klug, J. U. Becker, S. Mathey, K. Arefi, S. Balabanov, S. Venz, K.-H. Endlich, M. Pekna, J. E. Gessner, F. Thaiss, T. N. Meyer, Nephrotic syndrome and subepithelial deposits in a mouse model of immune-mediated anti-podocyte glomerulonephritis. *J. Immunol.* **187**, 3218–3229 (2011).
34. M. Van Roy, C. Ververken, E. Beirnaert, S. Hoefman, J. Kolkman, M. Vierboom, E. Breedveld, B. Hart, S. Poelmans, L. Bontinck, A. Hemeryck, S. Jacobs, J. Baumeister, H. Ulrichts, The preclinical pharmacology of the high affinity anti-IL-6R Nanobody® ALX-0061 supports its clinical development in rheumatoid arthritis. *Arthritis Res. Ther.* **17**, 135 (2015).
35. B. S. Khakh, R. A. North, P2X receptors as cell-surface ATP sensors in health and disease. *Nature* **442**, 527–532 (2006).
36. A. Elssner, M. Duncan, M. Gavrilin, M. D. Wewers, A novel $P2X_7$ receptor activator, the human cathelicidin-derived peptide LL37, induces IL-1β processing and release. *J. Immunol.* **172**, 4987–4994 (2004).
37. W. Nörenberg, H. Sobottka, C. Hempel, T. Plötz, W. Fischer, G. Schmalzing, M. Schaefer, *Positive allosteric modulation by ivermectin of human but not murine P2X7 receptors. Br. J. Pharmacol.* **167**, 48–66 (2012).
38. L.-H. Jiang, J. M. Baldwin, S. Roger, S. A. Baldwin, Insights into the molecular mechanisms underlying mammalian P2X7 receptor functions and contributions in diseases, revealed by structural modeling and single nucleotide polymorphisms. *Front. Pharmacol.* **4**, 55 (2013).
39. S. J. Fuller, L. Stokes, K. K. Skarratt, B. J. Gu, J. S. Wiley, Genetics of the $P2X_7$ receptor and human disease. *Purinergic Signalling* **5**, 257–262 (2009).
40. T. Li, J.-P. Bourgeois, S. Celli, F. Glacial, A.-M. Le Sourd, S. Mecheri, B. Weksler, I. Romero, P.-O. Couraud, F. Rougeon, P. Lafaye, Cell-penetrating anti-GFAP VHH and corresponding fluorescent fusion protein VHH-GFP spontaneously cross the blood-brain barrier and specifically recognize astrocytes: Application to brain imaging. *FASEB J.* **26**, 3969–3979 (2012).
41. C. Vincke, R. Loris, D. Saerens, S. Martinez-Rodriguez, S. Muyldermans, K. Conrath, General strategy to humanize a camelid single-domain antibody and identification of a universal humanized nanobody scaffold. *J. Biol. Chem.* **284**, 3273–3284 (2009).
42. F. Peyvandi, M. Scully, J. A. Kremer Hovinga, S. Cataland, P. Knöbl, H. Wu, A. Artoni, J.-P. Westwood, M. Mansouri Taleghani, B. Jilma, F. Callewaert, H. Ulrichts, C. Duby, D. Tersago; TITAN Investigators, Caplacizumab for acquired thrombotic thrombocytopenic purpura. *N. Engl. J. Med.* **374**, 511–522 (2016).
43. T. Schirrmann, K. Büssow, in *Antibody Engineering Volume 2*, R. E. Kontermann, S. Dübel, Eds. (Springer-Verlag Berlin Heidelberg, 2010), pp. 387–398.
44. J. Zhang, X. Liu, A. Bell, R. To, T. N. Baral, A. Azizi, J. Li, B. Cass, Y. Durocher, Transient expression and purification of chimeric heavy chain antibodies. *Protein Expression Purif.* **65**, 77–82 (2009).
45. F. Koch-Nolte, J. Reyelt, B. Schöβow, N. Schwarz, F. Scheuplein, S. Rothenburg, F. Haag, V. Alzogaray, A. Cauerhff, F. A. Goldbaum, Single domain antibodies from llama effectively and specifically block T cell ecto-ADP-ribosyltransferase ART2.2 in vivo. *FASEB J.* **21**, 3490–3498 (2007).
46. M. Seman, S. Adriouch, F. Scheuplein, C. Krebs, D. Freese, G. Glowacki, P. Deterre, F. Haag, F. Koch-Nolte, NAD-induced T cell death: ADP-ribosylation of cell surface proteins by ART2 activates the cytolytic P2X7 purinoceptor. *Immunity* **19**, 571–582 (2003).
47. S. Adriouch, P. Bannas, N. Schwarz, R. Fliegert, A. H. Guse, M. Seman, F. Haag, F. Koch-Nolte, ADP-ribosylation at R125 gates the P2X7 ion channel by presenting a covalent ligand to its nucleotide binding site. *FASEB J.* **22**, 861–869 (2008).
48. B. Rissiek, W. Danquah, F. Haag, F. Koch-Nolte, Technical Advance: A new cell preparation strategy that greatly improves the yield of vital and functional Tregs and NKT cells. *J. Leukoc. Biol.*, **95**, 543–549 (2014).
49. A. Baroja-Mazo, F. Martín-Sánchez, A. I. Gomez, C. M. Martínez, J. Amores-Iniesta, V. Compan, M. Barberà-Cremades, J. Yagüe, E. Ruiz-Ortiz, J. Antón, S. Buján, I. Couillin, D. Brough, J. I. Arostegui, P. Pelegrin, The NLRP3 inflammasome is released as a particulate danger signal that amplifies the inflammatory response. *Nat. Immunol.* **15**, 738–748 (2014).
50. D. P. Sester, S. J. Thygesen, V. Sagulenko, P. R. Vajjhala, J. A. Cridland, N. Vitak, K. W. Chen, G. W. Osborne, K. Schroder, K. J. Stacey, A novel flow cytometric method to assess inflammasome formation. *J. Immunol.* **194**, 455–462 (2015).

Acknowledgments: We thank B. Ziesch, M. Nissen, F. Seyfried, G. Dubberke, J. Schmid, and A. Kruse (Hamburg) and J. Noens, J. T'Syen, F. Calle, and J. Goncalves (Ablynx) for technical assistance. We thank H.-W. Mittrücker and B. Fleischer (Institute of Immunology, University Medical Center, Hamburg) and G. Hermans (Ablynx) for the critical reading of the manuscript. **Funding:** This study was supported in part by grants from the Deutsche Forschungsgemeinschaft (SFB1192-B5 to F.K.-N.; SFB1192-B3 to C.M.-S.; No310/8-1 to F.H. and F.K.-N.; No310/11-1 to F.K.-N.; and To235/6-1 to E.T.), by COST Action BM1406 (to F.K.-N.), by "NanoStroke" from the ERA-Net Neuron (to T.M., E.T., and F.K.-N.), by stipends from the Graduiertenkolleg of the SFB841 and SFB877 (to D.I., M.A., J.-H.K., and A.H.), by a grant from the Deutsche Akademische Austauschdienst (to C.P.), by a grant from the Werner Otto Foundation (to P. Bergmann), and by research funding from Ablynx NV (to F.K.-N.). **Author contributions:** W.D., B.R., D.I., N.S., C.P., M.A., and A.S.-P. cloned and purified Nanobodies and performed Ca^{2+} flux, DAPI uptake, ectodomain shedding, and IL-1β release assays. C.M.-S. supervised and performed the antipodocyte nephritis (APN) studies. J.-H.K. and A.H. performed the APN studies. P. Bergmann and E.B.-G. performed oocyte injections. J.A. cloned the phage display libraries and performed selections and primary screening of mouse P2X7–specific nanobodies, and W.R. cloned and produced monovalent and multivalent P2X7-specific nanobodies. F.H., E.T., P. Bannas, E.B.-G.,

and T.M. supervised the functional P2X7 assays and analyzed the data. T.L. and C.S. supervised the llama immunizations and lead discovery, as well as the setup of the APN studies, and analyzed the data. W.D., C.M.-S., B.R., and F.K.-N. assembled the figures. F.K.-N. supervised all of the research and wrote the manuscript, which was approved by all authors. **Competing interests:** J.A., W.R., T.L., and C.S. are or were employees of Ablynx NV and own shares and/or stock options with Ablynx NV. F.K.-N. and F.H. receive royalties from the sales of antibodies developed in their laboratories via MediGate GmbH, a 100% subsidiary of the University Medical Center, Hamburg. F.K.-N., W.D., C.S., J.A., and T.L. are co-inventors on patent applications on P2X7-specific nanobodies. The remaining authors declare that they have no competing interests. **Data and materials availability:** Nanobodies described in this paper can be obtained by academic researchers through a material transfer agreement.

Submitted 18 August 2015
Resubmitted 11 April 2016
Accepted 27 October 2016
Published 23 November 2016
10.1126/scitranslmed.aaf8463

Citation: W. Danquah, C. Meyer-Schwesinger, B. Rissiek, C. Pinto, A. Serracant-Prat, M. Amadi, D. Iacenda, J.-H. Knop, A. Hammel, P. Bergmann, N. Schwarz, J. Assunção, W. Rotthier, F. Haag, E. Tolosa, P. Bannas, E. Boué-Grabot, T. Magnus, T. Laeremans, C. Stortelers, F. Koch-Nolte, Nanobodies that block gating of the P2X7 ion channel ameliorate inflammation. *Sci. Transl. Med.* **8**, 366ra162 (2016).

Science Translational Medicine
AAAS

Nanobodies that block gating of the P2X7 ion channel ameliorate inflammation

Welbeck Danquah, Catherine Meyer-Schwesinger, Björn Rissiek, Carolina Pinto, Arnau Serracant-Prat, Miriam Amadi, Domenica Iacenda, Jan-Hendrik Knop, Anna Hammel, Philine Bergmann, Nicole Schwarz, Joana Assunção, Wendy Rotthier, Friedrich Haag, Eva Tolosa, Peter Bannas, Eric Boué-Grabot, Tim Magnus, Toon Laeremans, Catelijne Stortelers and Friedrich Koch-Nolte

(November 23, 2016)
Science Translational Medicine **8** (366), 366ra162. [doi: 10.1126/scitranslmed.aaf8463]

Editor's Summary

Tackling a tough target: An ATP-sensitive channel

Injured and dying cells release lots of ATP, which triggers inflammation by binding to the ion channel P2X7. Interfering with this process could treat numerous diseases, but so far small-molecule drugs have not been potent or specific enough. Now, Danquah and colleagues have developed single-domain "mini antibodies" called nanobodies that rise to the challenge. One of their nanobodies blocked the P2X7 channel and inhibited disease in mouse models of kidney inflammation and contact dermatitis. Another nanobody dampened the release of inflammatory messengers from human cells 1000 times more effectively than the small-molecule drugs now under development. Nanobodies can be linked together to prolong their lifetime or confer cell specificity, a useful versatility that increases their appeal.

Science Translational Medicine (print ISSN 1946-6234; online ISSN 1946-6242) is published weekly, except the last week in December, by the American Association for the Advancement of Science, 1200 New York Avenue, NW, Washington, DC 20005.